

GSA Data Repository Item for: “Resolving Milankovitchian Controversies: The Triassic Latemar Limestone and the Eocene Green River Formation”

Stephen R. Meyers Department of Geological Sciences, University of North Carolina at Chapel Hill, Chapel Hill, North Carolina 27599-3315, USA

1 INTRODUCTION

This GSA Data Repository Item contains supplemental information for the *Geology* publication “Resolving Milankovitchian Controversies: The Triassic Latemar Limestone and the Eocene Green River Formation” (Meyers, 2008). Topics addressed here include: (1) an introduction to the ASM methodology, (2) specific information pertaining to the analysis of the Latemar Limestone Cimon del Latemar (CDL) series (Preto et al., 2001), and the Green River Formation Currant Creek Ridge No. 1 (CCR-1) series (Roehler, 1991), and (3) an example illustrating application of the ASM method to a known *non-orbital* signal.

2 THE ASM METHODOLOGY

Average spectral misfit (ASM) is a statistical method to quantify the discrepancy between a target orbital spectrum, and the measured peaks in a stratigraphic spectrum, given a particular sedimentation rate. The metric is measured in cycles/k.y., and represents the average distance (or “misfit”) between the target and measured spectrum peaks, while also accounting for the resolution limits inherent in the analysis. ASM is defined as (Meyers and Sageman, 2007):

$$ASM = \frac{1}{N} \sum_{k=1}^N \alpha_k$$

$$\alpha_k = \begin{cases} 0 & \text{if } |(f^*s) - f_{pred}| \leq 0.5 * \Delta f_R * s \\ |(f^*s) - f_{pred}| & \text{if } |(f^*s) - f_{pred}| > 0.5 * \Delta f_R * s \end{cases}$$

N = number of orbital periods in the analysis

f = spatial frequency peak location (cycles/m)

s = sedimentation rate (m/k.y.)

f_{pred} = predicted orbital frequency (cycles/k.y.)

Δf_R = spatial frequency resolution bandwidth (cycles/m)

α_k = distance (in cycles/k.y.) between the location of the predicted orbital component and the closest significant peak in the spectrum (f^*s)

Orbital terms that lie above the Nyquist frequency or below the Rayleigh frequency are not evaluated, as they cannot be robustly detected. I use the harmonic test of

Thomson (1982) to identify significant spatial periods (f). Importantly, the minimum resolution bandwidth of these frequency estimates is approximately equivalent to the Rayleigh resolution (Thomson, 1990; Meyers and Sageman, 2007).

Significance levels for rejection of the null hypothesis (no orbital signal) are estimated with Monte Carlo spectra simulations. The simulated spectra have the same resolution limitations (Nyquist frequency and Rayleigh resolution) as the measured spectrum, but contain randomly distributed frequencies. ASM probability distributions for each temporal calibration are constructed using the simulated spectra. The null hypothesis (H_0) significance levels indicate how frequently a particular ASM value should occur by chance, given a spectrum with randomly distributed frequencies. Detailed information on the method can be found in Meyers and Sageman (2007).

3 DATA DESCRIPTION AND PREPARATION

The CDL lithofacies rank series of Preto et al. (2001) is the result of a continuous centimeter-scale analysis of the lagoonal carbonates at Cimon del Latemar, originally reported as bed thickness and rank (see Fig. DR1A). The series was sampled at an interval of 5 cm prior to spectral analysis. This sampling interval is sufficient to resolve all proposed orbital models.

The CCR-1 Fischer Assay data of Roehler (1991) was collected almost continuously through the Wilkins Peak Member, in sections of core that range from 0.12 m to 1.74 m, with an average thickness of 0.42 m (see Fig. DR1B). Oil yield values were assigned to the middle of each sample interval. The resulting data set has an average sampling interval of 0.5 m. Approximately 71% of the data set is characterized by a sampling interval of less than 1 m. I utilize the latter value for a conservative estimate of the Nyquist frequency (0.5 cycles/m).

Much attention has been brought to bear on the issue of how to analyze unevenly sampled data, since interpolation can potentially introduce bias. One option is utilize spectrum estimation techniques that directly process unevenly sampled data

(Scargle, 1982). Another approach to this problem is to preserve the detailed shape of the time series by interpolating on an extremely fine sampling grid. To preserve its fine scale structure, the CCR-1 Fischer Assay data was linearly interpolated to a sampling interval of 0.1 m prior to analysis. Despite this high-resolution sampling, the spectral results are only interpreted within the frequency range of 0 cycles/m to 0.5 cycles/m.

4 SPECTRAL ANALYSIS

Following removal of the mean value and a linear trend from each data series, multitaper method (MTM) spectral analysis was conducted using three 2π tapers (Thomson, 1982). The power spectral estimates utilize an iterative adaptive weighting procedure (Thomson, 1982). Reported power estimates have been normalized by the number of data points each stratigraphic data series.

5 ASM ANALYSIS

For both the CDL and CCR-1 data series, the average spectral misfit analysis was conducted using all significant harmonic components with $\geq 90\%$ probability. The predicted orbital parameters of Berger et al. (1992) and Berger and Loutre (1991) were utilized for the target orbital spectra. For the Triassic (241.5 m.y.) these orbital periods are: 404.18 k.y., 123.82 k.y., 94.78 k.y., 45.29 k.y., 35.77 k.y., 21.25 k.y., 17.75 k.y. For the Eocene (50 m.y.) these orbital periods are: 404.18 k.y., 123.82 k.y., 94.78 k.y., 52.10 k.y., 39.90 k.y., 22.60 k.y., 18.80 k.y. Although the precession and obliquity terms for the Triassic and Eocene are characterized by shorter periods than their Quaternary values, deviation of the eccentricity periods from their modern values is expected to be negligible (Berger et al., 1992).

The null hypothesis Monte Carlo tests employed 100,000 randomly organized spectra, with the number of significant frequencies equivalent to that of the measured spectra. All orbital configurations were investigated. In both the CDL and CCR-1 series, the orbital configuration with the lowest H_0 significance level contained the precession, obliquity and eccentricity terms.

5.1 NOTES ON THE ANALYSIS OF THE LATEMAR LIMESTONE CDL SERIES

Figures DR2 and DR3 provide supplemental information about the analysis of the Latemar Limestone CDL series displayed in Figure 1 (see main article). In addition to the H_0 significance levels previously shown, Figure DR2 displays the ASM values for each sedimentation rate, and the number of orbital terms available for ASM calculation.

Figure DR3 illustrates the fit between the target orbital spectrum and the measured spectrum for three proposed orbital interpretations: Kent et al. (2004) = 50 cm/k.y.; Zuehlke et al. (2003) = 25 cm/k.y.; Preto et al. (2001) = 4.85 cm/k.y. The target orbital spectrum for the 50 cm/k.y. calibration does not include the long eccentricity term (404.18 k.y.), as this component falls below the temporal Rayleigh frequency and thus cannot be robustly detected. The horizontal “whisker” bars at the top of the measured spectral peaks in Figure DR3 indicate their temporal frequency resolution bandwidth. This resolution bandwidth decreases with sedimentation rate. Monte Carlo spectra simulations identify an optimal sedimentation rate of 4.85 cm/k.y.

5.2 NOTES ON THE ANALYSIS OF THE GREEN RIVER FORMATION CCR-1 SERIES

Figures DR4-DR6 provide supplemental information about the analysis of the Green River Formation CCR-1 series displayed in Figure 2 (see main article). In addition to the H_0 significance levels previously shown, Figure DR4 displays the ASM values for each sedimentation rate, and the number of orbital terms available for ASM calculation.

Figure DR5 illustrates the fit between the target spectrum and measured spectrum for three potential sedimentation rates: 35.00 cm/k.y., 16.95 cm/k.y., and 4 cm/k.y. The target orbital spectrum for the 4 cm/k.y. calibration does not include the precession terms (22.60 k.y., 18.80 k.y.) nor the short obliquity term (39.90 k.y.), as these components exceed the temporal Nyquist frequency and thus cannot be robustly detected. As in figure DR3, the horizontal “whisker” bars at the top of the measured spectral peaks in Figure DR5 indicate their temporal frequency resolution bandwidth. Monte Carlo spectra simulations identify an optimal sedimentation rate of 16.95 cm/k.y.

Figure DR6 and Figure 2 of the main text illustrate an important aspect of the ASM method. As previously shown in Figure 2D, investigation of sedimentation rates from 3.5-5 cm/k.y. identifies a number of distinct H_0 significance level minima not apparent in

the coarse-resolution analysis (Fig. 2C). In contrast, the results from 16 to 17.5 cm/k.y. more smoothly vary, and reflect the global minimum apparent in Figure 2C. This is a consequence of the fact that ASM (cycles/k.y.) can vary rapidly at very low sedimentation rates. Investigation of sedimentation rates from 1 to 20 cm/k.y. (with a 0.05 cm/k.y. increment) further demonstrates this characteristic of the method (Fig. DR6).

The cause of the rapid ASM variability at low sedimentation rates is twofold. Foremost, as sedimentation rate decreases the effective length of the time series increases, resulting in a smaller temporal frequency resolution bandwidth (cycles/k.y.). This naturally increases the sensitivity of the spectrum. In addition to this factor, the temporal Nyquist frequency (cycles/k.y.) decreases with sedimentation rate, which can result in a rapid loss of orbital terms available for ASM calculation. These factors must be carefully considered in any analysis.

6. ANALYSIS OF A NON-ORBITAL SIGNAL

Cyclostratigraphic models have been previously utilized to demonstrate the ASM technique (see Meyers and Sageman, 2007). As a complimentary exercise, this section illustrates how the method responds to data that *clearly do not* contain an orbital signal. Herein I investigate an ~4 meter long reflectance (550 nm) data series from the Cariaco Basin previously published by Peterson et al. (2000) (Figure DR7A). This data series spans 0-10,980 years before present (Peterson et al., 2000).

Theoretically, what should the ASM results of this record to look like? Any cyclic stratigraphic record (orbitally derived or not) will be characterized by potential timescales that yield better or poorer fit to an orbital target. Furthermore, as the number of sedimentation rates analyzed increases, the likelihood of a identifying a “false positive” (an erroneous rejection of the null hypothesis) also increases. For example, if 100 independent sedimentation rates are investigated, we can expect one ASM value that reaches the 1% H_0 significance level purely by chance. It is therefore crucial to establish a threshold that accounts for such chance occurrences. This threshold is known as the “critical significance level”, and is defined as (Meyers and Sageman, 2007):

$$\text{Critical Significance Level} = \left(\frac{1}{\# \text{ Sedimentation Rates}} \right) * 100$$

As a rule of thumb, I typically investigate ~100 or more individual sedimentation rates

in each ASM analysis, yielding critical significance levels $\leq 1\%$.

MTM spectral analysis of the Cariaco reflectance series (using three 2π tapers) identifies 20 significant harmonic components with $\geq 90\%$ probability (Fig. DR7B). ASM analysis is conducted across sedimentation rates from 0.01-21.21 cm/k.y. (0.1 cm/k.y. step), using the target orbital spectrum developed for the Green River Formation CCR-1 data (selection of this particular target spectrum is arbitrary). Given the resolution limitations of the data, these sedimentation rates span the full range over which orbital forcing can reasonably be detected (Fig. DR7F). This approach is appropriate because we are blindly prospecting for an orbital signal in the Cariaco data. That is, for this exercise, we assume that no supplementary temporal constraints are available. Note that the sedimentation rates investigated here are not realistic, since the true measured (compacted) sedimentation rate is 35-38 cm/k.y. (Peterson et al., 2000).

As expected, the ASM results (Fig. DR7D) identify a number potential timescales that yield a superior fit to the orbital target. Given the resolution limitations of the Cariaco reflectance series, we observe a perfect fit (ASM = 0 cycles/k.y.) for sedimentation rates from 15.21-21.21 cm/k.y. In addition, relatively low ASM values ($\leq 5 \times 10^{-3}$ cycles/k.y.) occur at sedimentation rates from 0.01-1.41 cm/k.y., and 6.01-7.81 cm/k.y. But what is the likelihood that these observed ASM values are derived from a randomly organized spectrum?

Although the sedimentation rates from 15.21-21.21 cm/k.y. are characterized by a perfect fit to the orbital target, these timescales yield relatively high H_0 significance levels ($>9.6\%$; Fig. DR7E). This result indicates that $>9.6\%$ of the Monte Carlo spectra simulations yield a perfect fit to the detectable orbital terms (two or less; Fig. DR7F). The minimum H_0 significance level observed in the entire analysis is at 7.01 cm/k.y. (2.15%; Fig. DR7E). Given the analysis of 212 independent sedimentation rates, we can expect approximately one value that reaches the 0.47% H_0 significance level purely by chance. None of the investigated sedimentation rates exceed this critical significance level. Thus, the null hypothesis (no orbital forcing) cannot be rejected with a high degree of confidence. That is, the ensemble of significant frequency components observed in the Cariaco reflectance data cannot be aligned to the orbital frequencies any better than randomly organized spectra.

7. REFERENCES

- Berger, A., and Loutre, M., 1991, Insolation values for the climate of the last 10 million years: *Quaternary Science Reviews*, v. 10, p. 297–317.
- Berger, A., Loutre, M.F., and Laskar, J., 1992, Stability of the astronomical frequencies over the Earth's history for paleoclimate studies: *Science*, v.255, p. 560–566.
- Kent, D.V., Muttoni, G., and Brack, P., 2004, Magnetostratigraphic confirmation of a much faster tempo for sea-level change for the Middle Triassic Latemar platform carbonates: *Earth and Planetary Science Letters*, v. 228, p. 369–377.
- Meyers, S.R., 2008, Resolving Milankovitchian Controversies: The Triassic Latemar Limestone and the Eocene Green River Formation: *Geology*.
- Meyers, S.R., and Sageman, B.B., 2007, Quantification of deep-time orbital forcing by average spectral misfit: *American Journal of Science*, v. 307, p. 773–792.
- Peterson, L.C., Haug, G.H., Hughen, K.A., and Rohl, U., 2000, Rapid changes in the hydrologic cycle of the tropical Atlantic during the last glacial: *Science*, v. 290, p. 1947–1951.
- Preto, N., Hinnov, L.A., Hardie, L.A., and De Zanche, V., 2001, Middle Triassic orbital signature recorded in the shallow-marine Latemar carbonate buildup (Dolomites, Italy): *Geology*, v. 29, p. 1123–1126.
- Roehler, H.W., 1991, Correlation and depositional analysis of oil shale and associated rocks in the Eocene Green River Formation, Greater Green River Basin, Southwest Wyoming: USGS Miscellaneous Investigations Series MAP I-2226.
- Scargle J.D., 1982, Studies in astronomical times series analysis. II Statistical aspects of spectral analysis of unevenly spaced data: *The Astrophysical Journal*, v. 263, p. 835–853.
- Thomson, D.J., 1982, Spectrum estimation and harmonic analysis: *IEEE Proceedings*, v. 70, p. 1055–1096.
- Thomson, D.J., 1990, Quadratic-inverse spectrum estimates: applications to palaeoclimatology: *Philosophical Transactions of the Royal Society of London. Series B, Biological Sciences*, v. 332, p. 539–597.
- Zuehlke, R., Bechstadt, T., and Mundil, R., 2003, Sub-Milankovitch and Milankovitch forcing on a model Mesozoic carbonate platform- the Latemar (Middle Triassic, Italy): *Terra Nova*, v. 15, p. 69–80.

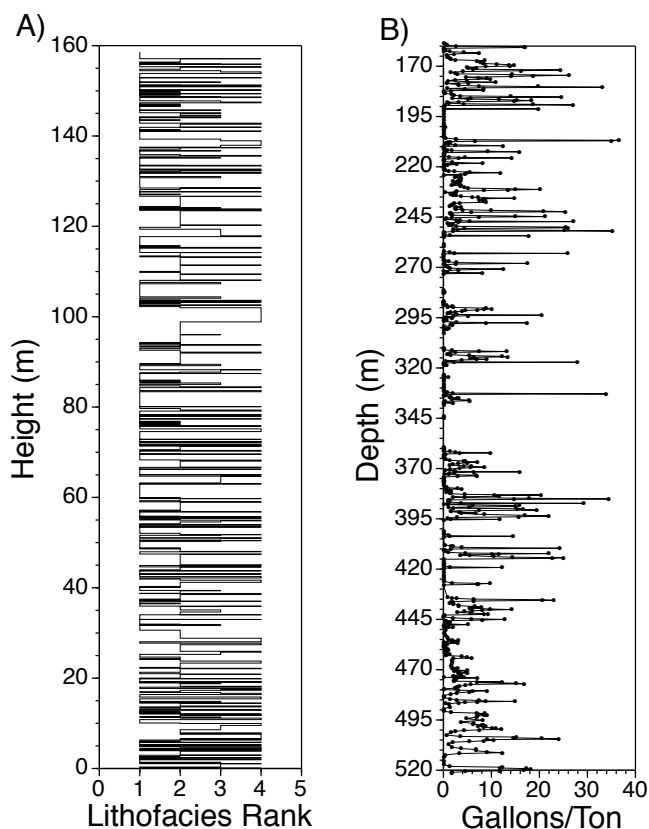


Figure DR1. A) The continuous Cimon del Latemar (CDL) lithofacies rank series from the Latemar Limestone (Dolomites, Italy) (Preto et al., 2001). B) Fischer Assay data (gallons of oil per ton of rock) spanning the Wilkins Peak Member of the Green River Formation, from the Currant Creek Ridge No. 1 core (Wyoming, USA) (Roehler, 1991).

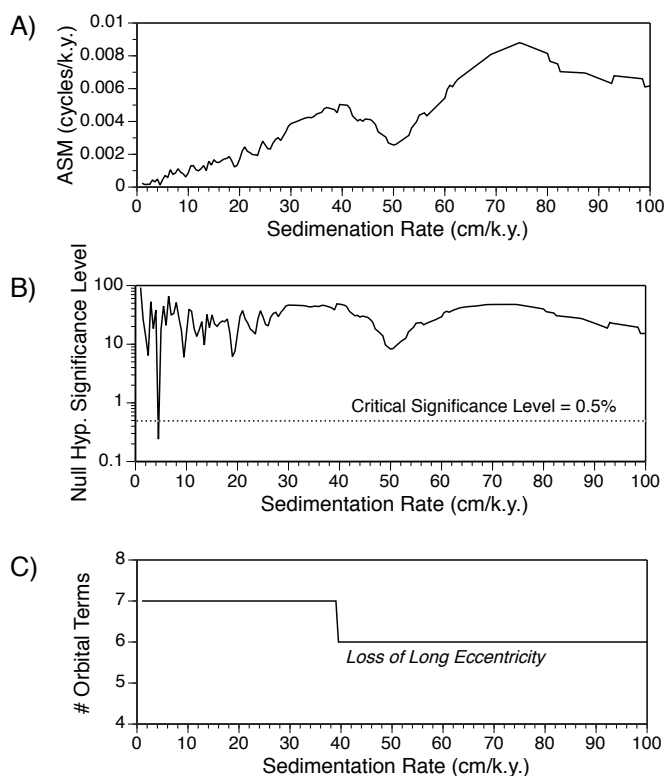


Figure DR2. Average spectral misfit results for the Latemar CDL Lithofacies series (Preto et al., 2001), across sedimentation rates from 1-100 cm/k.y., with an increment of 0.5 cm/k.y. A) Average spectral misfit in cycles/k.y. B) Null hypothesis significance levels. The dotted line indicates the critical significance level. C) The number of orbital terms available for ASM analysis.

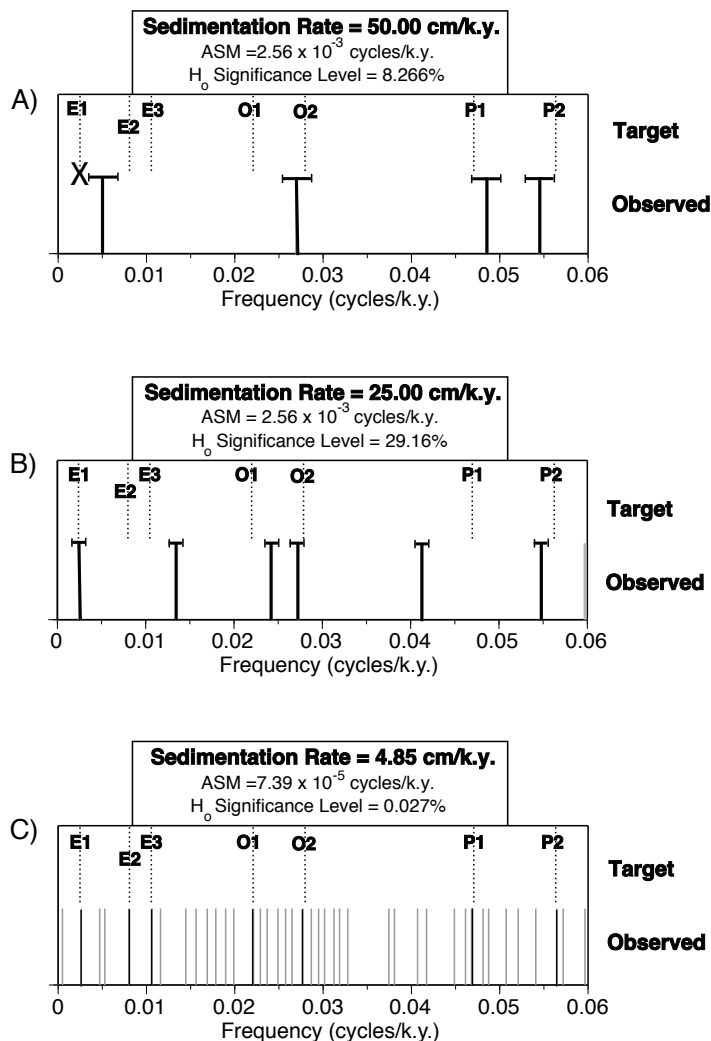


Figure DR3. A) The fit between the target orbital spectrum and the CDL measured spectrum, given a sedimentation rate of 50 cm/k.y. B) The fit between the target orbital spectrum and the measured spectrum, given a sedimentation rate of 25 cm/k.y. C) The fit between the target orbital spectrum and the measured spectrum, given a sedimentation rate of 4.85 cm/k.y. The measured peaks closest to the orbital target signals are indicated as black vertical lines, and all other peaks are indicated in gray. The horizontal "whisker" bars in part A and B illustrate the temporal frequency resolution bandwidth. Vertical dotted lines identify the target orbital signals.

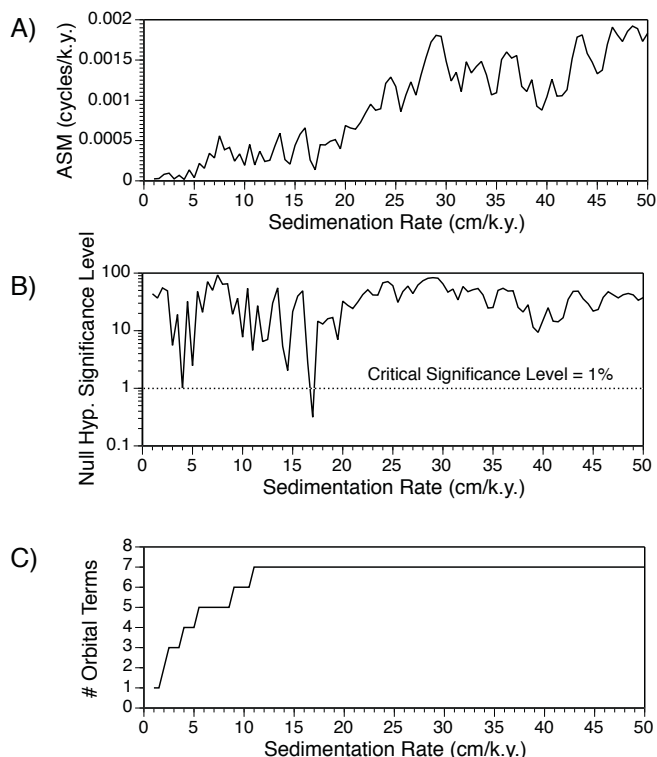


Figure DR4. Average spectral misfit results for the Green River Formation CCR-1 Fischer Assay data series (Roehler, 1991), across sedimentation rates from 1-50 cm/k.y., with an increment of 0.5 cm/k.y. A) Average spectral misfit in cycles/k.y. B) Null hypothesis significance levels. The dotted line indicates the critical significance level. C) The number of orbital terms available for ASM analysis.

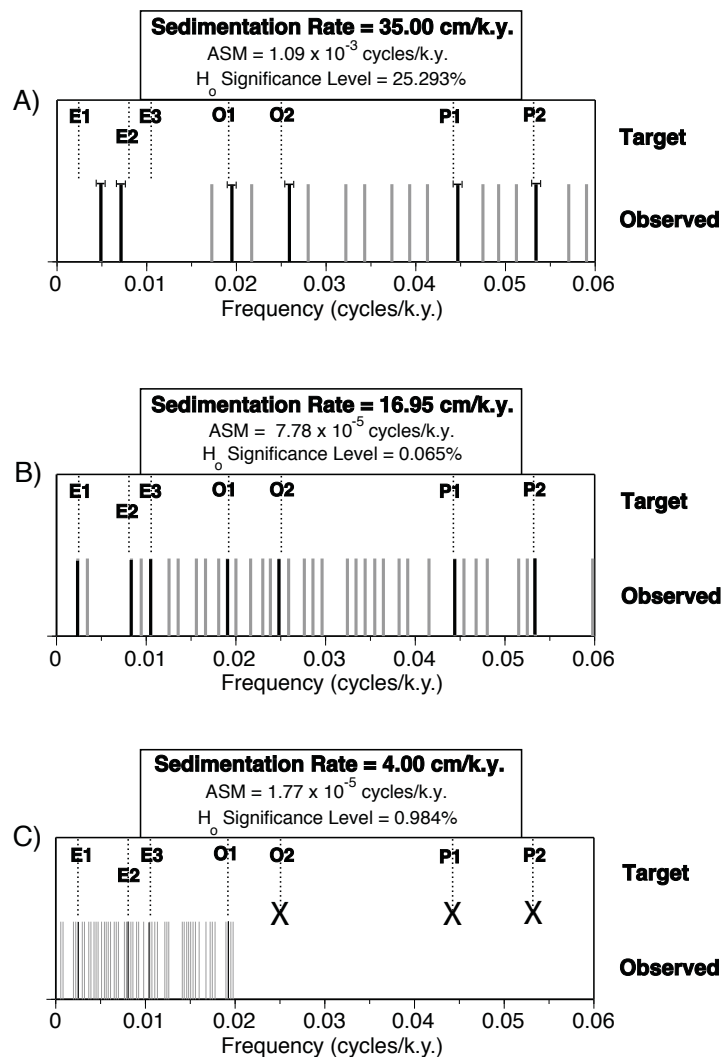


Figure DR5. A) The fit between the target orbital spectrum and the CCR-1 measured spectrum, given a sedimentation rate of 35 cm/k.y. B) The fit between the target orbital spectrum and the CCR-1 measured spectrum, given a sedimentation rate of 16.95 cm/k.y. C) The fit between the target orbital spectrum and the CCR-1 measured spectrum, given a sedimentation rate of 4 cm/k.y. The measured peaks closest to the orbital target signals are indicated as black vertical lines, and all other peaks are indicated in gray. The horizontal "whisker" bars in part A illustrate the temporal frequency resolution bandwidth. Vertical dotted lines identify the target orbital signals.

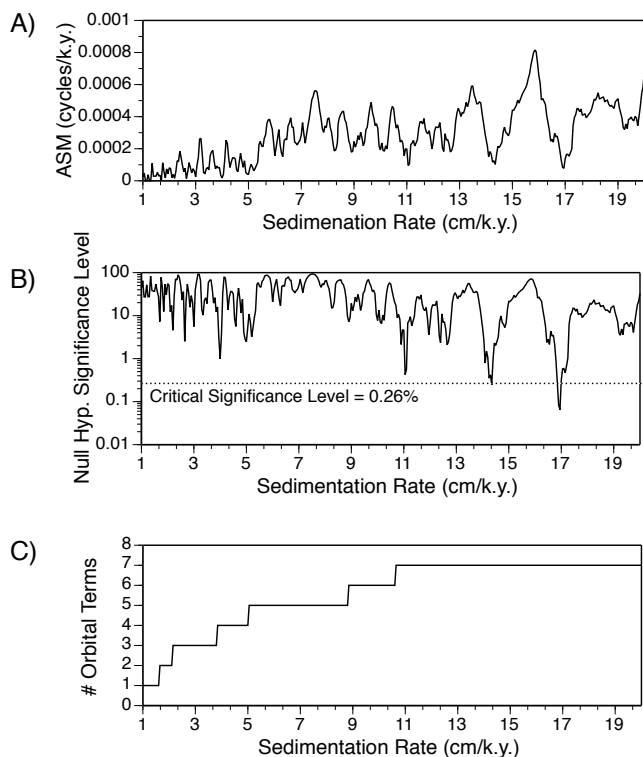


Figure DR6. Average spectral misfit results for the Green River Formation CCR-1 Fisher Assay data series (Roehler, 1991), across sedimentation rates from 1-20 cm/k.y., with an increment of 0.05 cm/k.y. A) Average spectral misfit in cycles/kyr. B) Null hypothesis significance levels. The dotted line indicates the critical significance level. C) The number of orbital terms available for ASM analysis.

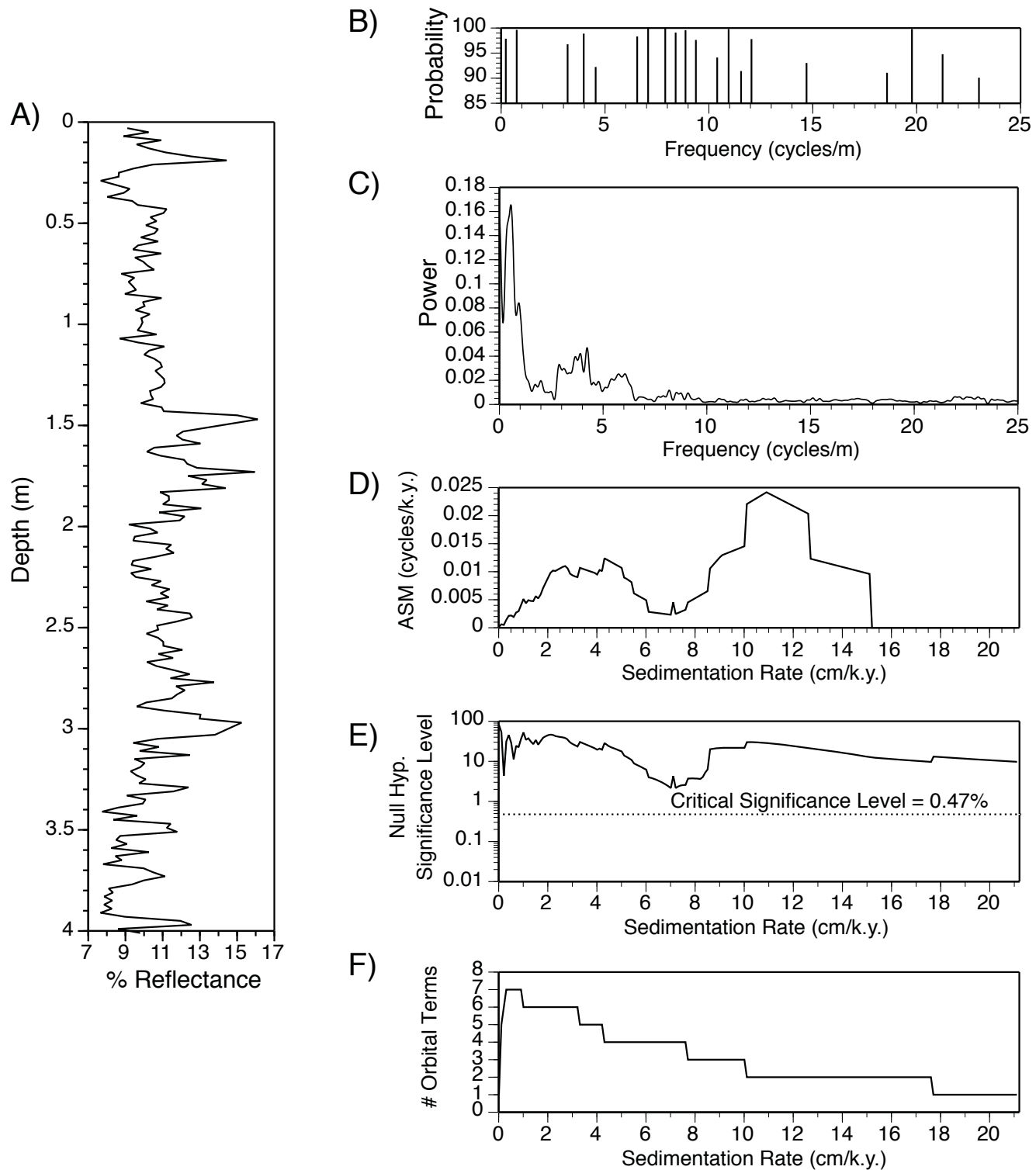


Figure DR7. Multitaper method spectral analysis and ASM results for the Cariaco reflectance (550 nm) data series (Peterson et al., 2000). MTM spectral analysis was conducted using three 2π tapers. A) The ~4 meter long Cariaco reflectance (550 nm) series. B) MTM harmonic analysis probability results. C) MTM power spectrum estimate. D) Average spectral misfit for sedimentation rates from 0.01 to 21.21 cm/k.y., calculated with a 0.1 cm/k.y. increment. E) Null hypothesis significance levels. The dotted line indicates the critical significance level. F) The number of orbital terms available for ASM analysis.